

## SOLUTION OF THE DIRECT ALLOY SOLIDIFICATION PROBLEM INCLUDING THE PHENOMENON OF MATERIAL SHRINKAGE

by

**Edyta HETMANIOK\***, **Damian SLOTA**, and **Adam ZIELONKA**

Institute of Mathematics, Silesian University of Technology,  
Gliwice, Poland

Original scientific paper  
DOI:10.2298/TSCI160405239H

*In the paper, we describe the solution technique for solving the direct problem of the alloy solidifying within the casting mould with the phenomenon of material shrinkage taken into account. Due to the difference between densities of the liquid and solid phases, the shrinkage of metal often appears during the solidification. The investigated process is modeled by means of the solidification in the temperature interval basing on the heat conduction equation with the source element enclosed which includes the latent heat of fusion and the volume contribution of solid phase. Whereas the shrinkage of metal is modeled by the proper application of the mass balance equation.*

Key words: *solidification, binary alloy, solidification in the temperature interval, shrinkage of metal.*

### Introduction

In the paper, we describe the method of solving the direct problem of the alloy solidifying within the casting mould with the phenomenon of material shrinkage taken into account. Due to the difference between densities of the liquid and solid phases, the shrinkage of metal often appears during the solidification. Then, between the cast and the casting mould the air gap may form which generates the interfacial thermal resistance between the mould and the cast. The created thermal resistance determines then the mould heat flux which, in result, decreases the quality of the product causing some defects, such as cracks or oscillation marks.

Creation of the heat resistance of the air gap between the ingot and crystallizer in the continuous casting process was investigated, for example, by Nawrat and Skorek [1] and Nawrat *et al.* [2]. For modeling the solidification process the authors used the Stefan problem and, on the basis of temperature measurements in the crystallizer walls, they determined the heat conduction coefficient of the gap. The heat resistance of the gap between the crystallizer, or the mould, and the ingot was also determined in papers [3, 4], whereas the interfacial heat transfer coefficient between the form and the cast was computed in works [5, 6].

One of the authors of the current paper obtained also some preliminary results in investigating the phenomenon of metal shrinkage in the solidification process modeled by means of the 1-D Stefan problem [7, 8]. The Stefan problem is the name of the wide class of mathematical models describing the thermal processes characterized by the phase transitions and it

\* Corresponding author, e-mail: edyta.hetmaniok@polsl.pl

is commonly used for modeling various problems concerning the solidification of pure metals [9-11]. Process investigated in this paper concerns however the solidification of alloy, therefore it is modeled with the aid of the so-called solidification in the temperature interval. In the Stefan model the liquid and solid phases are sharply separated by the interphase surface, whereas the solidification in the temperature interval model assumes the existence of the intermediate zone (called the mushy zone) between the liquid and solid phases where both phases coexist [12]. The used model is based on the heat conduction equation with the enclosed source element including the latent heat of fusion and the volume contribution of solid phase [13-16]. For the assumed form of function describing this contribution, the equation is transformed to the heat conduction equation with the so-called substitute thermal capacity. Thereby the considered differential equation describes the heat conduction in the full homogeneous region (in solid phase, in two-phase zone and in liquid phase).

Goal of the paper is to propose a procedure for solving the 1-D direct problem of the alloy solidification, that is to determine the temperature distribution in the investigated domain including the region of the ingot and the region of the casting mould, as well as the change of cast size associated with the material shrinkage. Technically the approach is based on the finite difference method supplemented by the procedure of correcting the field of temperature in the vicinity of the liquidus and solidus curves [15-17]. Whereas the shrinkage of metal is modeled by the proper application of the mass balance equation. Presentation of the proposed approach is supported by the results of the computational experiments illustrating the effectiveness and usefulness of the elaborated method.

### Governing equations

Let us consider the plate of thickness,  $d(t)$ , width,  $h$ , and height,  $l$ , (we assume  $d(t) \ll h$  and  $d(t) \ll l$ ) occupied by the solidifying material,  $\Omega$ , and bounded by the casting mould,  $\Omega_m$ . Scheme of the discussed region is presented in fig. 1. During the solidification process

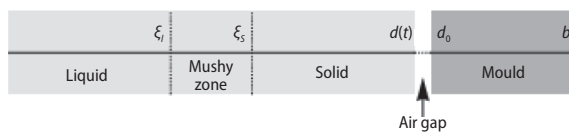


Figure 1. Region of the problem

the air gap appears between cast and the casting mould, thus in the initial moment  $d(0) = d_0$ . We assume in our analysis that the natural convection in the liquid phase as well as the strain energy of the mushy zone are neglected.

In region  $\Omega = \{(x,t) : x \in [0, d(t)], t \in (0, t^*)\}$  the distribution of temperature in the solidifying material is expressed by means of the following heat conduction equation:

$$c\rho \frac{\partial T(x,t)}{\partial t} + v_x \frac{\partial T(x,t)}{\partial x} = \lambda \frac{\partial^2 T(x,t)}{\partial x^2} + L\rho \frac{\partial f_s(x,t)}{\partial t}, \quad (x,t) \in \Omega, \quad (1)$$

where  $c$ ,  $\rho$ , and  $\lambda$  are the specific heat, mass density, and thermal conductivity coefficient, respectively,  $v_x$  – the velocity,  $L$  – the latent heat of solidification,  $f_s$  – the volumetric solid phase fraction,  $T$  – the temperature, and finally  $t$  and  $x$  refer to the time and spatial co-ordinates, respectively. The volumetric solid state fraction depends on the temperature, so we get:

$$\frac{\partial f_s}{\partial t} = \frac{\partial f_s}{\partial T} \frac{\partial T}{\partial t} \quad (2)$$

Substituting relation (2) to (1) and transforming the obtained equation we have:

$$\left(c - L \frac{\partial f_s}{\partial T}\right) \rho \frac{\partial T(x,t)}{\partial t} + v_x \frac{\partial T(x,t)}{\partial x} = \lambda \frac{\partial^2 T(x,t)}{\partial x^2} \quad (3)$$

By introducing the so-called substitute thermal capacity:

$$C = c - L \frac{\partial f_s}{\partial T} \quad (4)$$

the previous equation can be written in the form:

$$C \rho \frac{\partial T(x,t)}{\partial t} + v_x \frac{\partial T(x,t)}{\partial x} = \lambda \frac{\partial^2 T(x,t)}{\partial x^2}, \quad (x,t) \in \Omega \quad (5)$$

By assuming the linear variation of function  $f_s$  with respect to temperature, then, since the following equalities must be satisfied:

$$f_s(T_L) = 0 \quad \text{and} \quad f_s(T_S) = 1 \quad (6)$$

where  $T_L$  and  $T_S$  denote the liquidus and solidus temperatures, respectively, we obtain:

$$f_s(T) = \frac{T_L - T}{T_L - T_S} \quad \text{for} \quad T \in [T_S, T_L] \quad (7)$$

A number of various hypothesis concerning the form of function  $f_s$ , describing the volumetric solid state fraction, can be found in literature. One of the possibilities is to assume the linear dependence of the solid phase on the temperature in the mushy zone [14-16] which, together with the previous described conditions, results in the form of relation (7). Differentiating this function, we get:

$$\frac{df_s(T)}{dT} = \frac{-1}{T_L - T_S} \quad \text{for} \quad T \in [T_S, T_L] \quad (8)$$

Hence, the substitute thermal capacity is equal to:

$$C = \begin{cases} c_l & T > T_L, \\ c_{mz} + \frac{L}{T_L - T_S} & T \in [T_S, T_L], \\ c_s & T < T_S, \end{cases} \quad (9)$$

where  $c_l$ ,  $c_m$ , and  $c_s$  denote the specific heat of the liquid phase, mushy zone, and the solid phase, respectively. In eq. (5) the values of density and thermal conductivity coefficient vary as well in dependence on the temperature:

$$\rho = \begin{cases} \rho_l & T > T_L, \\ \rho_{mz} & T \in [T_S, T_L], \\ \rho_s & T < T_S, \end{cases} \quad \lambda = \begin{cases} \lambda_l & T > T_L, \\ \lambda_{mz} & T \in [T_S, T_L], \\ \lambda_s & T < T_S. \end{cases} \quad (10)$$

The substitute thermal capacity, density, and thermal conductivity coefficient of the mushy zone depend on the solid phase contribution  $f_s$  in the following way:

$$\begin{aligned}c_{mz} &= c_l(1 - f_s) + c_s f_s, \\ \rho_{mz} &= \rho_l(1 - f_s) + \rho_s f_s, \\ \lambda_{mz} &= \lambda_l(1 - f_s) + \lambda_s f_s\end{aligned}\quad (11)$$

In region  $\Omega_m = \{(x, t) : x \in (d_0, b), t \in (0, t^*)\}$  of the casting mould the distribution of temperature is described by equation:

$$c_m \rho_m \frac{\partial T_m(x, t)}{\partial t} = \lambda_m \frac{\partial^2 T_m(x, t)}{\partial x^2}, \quad (x, t) \in \Omega_m \quad (12)$$

where  $c_m$ ,  $\rho_m$ , and  $\lambda_m$  are the specific heat, mass density, and thermal conductivity coefficient, respectively, of the casting mould material, and  $T_m$  – the temperature of casting mould.

The previous equations are completed by the following initial conditions:

$$T(x, 0) = T_0(x), \quad x \in [0, d_0] \quad (13)$$

where  $T_0(x) > T_L$  (the cast is at the beginning in the liquid phase) and

$$T_m(x, 0) = T_{m,0}(x), \quad x \in [d_0, b] \quad (14)$$

of course the consistency condition  $T_0(d) = T_{m,0}(d_0)$  must hold as well as the boundary conditions:

$$-\lambda_l \frac{\partial T(0, t)}{\partial x} = 0, \quad t \in (0, t^*) \quad (15)$$

$$-\lambda_m \frac{\partial T_m(b, t)}{\partial x} = \alpha [T_m(b, t) - T_\infty], \quad t \in (0, t^*) \quad (16)$$

where  $\alpha$  is the heat transfer coefficient and  $T_\infty$  – the ambient temperature.

At the beginning of the solidification process there is no any air gap, it creates while the material solidifies, so in contact of the cast and the casting mould we define the fourth kind boundary condition in two forms:

– with no air gap (the perfect contact)

$$-\lambda_l \frac{\partial T(d_0, t)}{\partial x} = -\lambda_m \frac{\partial T_m(d_0, t)}{\partial x} \quad (17)$$

– with the air gap

$$-\lambda_s \frac{\partial T[d(t), t]}{\partial x} = \frac{T[d(t), t] - T_m(d_0, t)}{R} = -\lambda_m \frac{\partial T_m(d_0, t)}{\partial x} \quad (18)$$

where  $R = [d_0 - d(t)]/\lambda_g$  describes the thermal resistance with  $\lambda_g$  denoting the thermal conductivity coefficient of the air gap.

Now let us assume that the total mass of the material is equal to  $m_0$  and it is constant during the time of modelled process. By denoting the masses of material in the liquid, solid, and intermediate (mushy zone) states as  $m_l$ ,  $m_s$ , and  $m_{mz}$ , respectively, we may formulate the mass balance equation:

$$m_0 = m_l + m_{mz} + m_s \quad (19)$$

from which, after including the notation introduced in fig. 1, we get the relation:

$$\rho_l d_0 hl = \rho_l \xi_l hl + \rho_{mz} (\xi_s - \xi_l) hl + \rho_s [d(t) - \xi_s] hl \quad (20)$$

After simple transformations we obtain the formula determining the width of the cast in dependence of time:

$$d(t) = \xi_s + \frac{\rho_l}{\rho_s} (d_0 - \xi_l) - \frac{\rho_{mz}}{\rho_s} (\xi_s - \xi_l) \quad (21)$$

Before appearing of the solid state, it means when the mass balance equation has the form:

$$m_0 = m_l + m_{mz} \quad (22)$$

that is:

$$\rho_l d_0 hl = \rho_l \xi_l hl + \rho_{mz} [d(t) - \xi_l] hl \quad (23)$$

the width of the cast is expressed by the following equation :

$$d(t) = \xi_l + \frac{\rho_l}{\rho_{mz}} (d_0 - \xi_l) \quad (24)$$

### Method of solution

The investigated problem is solved by using the implicit scheme of finite difference method, with the appropriate approximation of the boundary conditions, supplemented by the procedure of correcting the field of temperature in the vicinity of liquidus and solidus curves. Let us present the short description of this method. More detailed version, as well as its generalization, can be found in literature [15-17].

In the cast region and in the mould region two following different meshes are introduced:

$$\Delta_{cast} = \left\{ x_i = i \cdot k_{cast}; \quad k_{cast} = \frac{d_0}{n_{cast}}; \quad i = 0, 1, \dots, \left[ \frac{d(t)}{k_{cast}} \right] \right\} \cup \{d(t)\},$$

$$\Delta_{mould} = \left\{ x_j = d_0 + j \cdot k_{mould}; \quad k_{mould} = \frac{b - d_0}{n_{mould}}; \quad j = 0, 1, \dots, n_{mould} \right\}$$

where  $[\cdot]$  denotes the integer part. It means that the nodes are placed with the constant step, except the last node in the cast region which is always equal to  $d(t)$ . When the solidification process proceeds, the number of nodes in the cast changes according to the previous relation.

Distribution of temperature in moment  $t_{p+1}$ , in the cast as well as in the mould, is determined on the way of solving the proper system of equations with the aid of finite difference method. Next, the value of temperature in moment  $t_{p+1}$  in the node  $x_i$  of the cast is corrected by using the following procedure. If the node  $x_i$  in moment  $t_p$  was in the liquid phase, its temperature  $T_i^p$  was greater than the liquidus temperature,  $T_L$ . Thus, to execute the next step of calculations we should use for this node the values of parameters corresponding to the liquid phase. If temperature  $T_i^{p+1}$  in this node, obtained for the next moment  $t_{p+1}$ , is still greater than the liquidus temperature,  $T_L$ , then the node still remains in the liquid phase, so the temperature  $T_i^{p+1}$  can be accepted as properly determined and does not require any more attention.

However, if the new calculated temperature  $T_i^{p+1}$  is lower than the liquidus temperature,  $T_L$ , it means that the node passes to another phase (mushy zone or solid phase), therefore the values of the thermal parameters should change, properly to the new phase. Let us assume that  $T_i^{p+1} \in (T_S, T_L]$ , which means that the node passes to the mushy zone. Change of the phase by the node happened in time  $\Delta t = t_{p+1} - t_p$ , so for part of this time the values of parameters should correspond to the new phase, and therefore the temperature in node  $x_i$  should be corrected. We use for this goal the energy balance relation for the control element  $V_i$  with central node  $x_i$ . Change of enthalpy of this element, connected with its cooling from temperature  $T_i^p$  to temperature  $T_i^{p+1}$ , is equal to:

$$\Delta H_i = C_l \rho_l (T_i^p - T_i^{p+1}) \Delta V_i$$

where  $C_l$  is the substantial thermal capacity of the liquid phase and  $\rho_l$  – the density of the liquid phase. In real the loss of this heat performs in two stages. The first stage is connected with the cooling to the liquidus temperature,  $T_L$ , and the second stage – with the cooling from the liquidus temperature,  $T_L$ . Thus, we have two equalities:

$$\Delta H_{i1} = C_l \rho_l (T_i^p - T_L) \Delta V_i$$

$$\Delta H_{i2} = C_{mz} \rho_{mz} (T_L - \bar{T}_i^{p+1}) \Delta V_i$$

where  $C_m$  is the substantial thermal capacity of the mushy zone,  $\rho_{mz}$  – the density of the mushy zone, and whereas  $\bar{T}_i^{p+1}$  – the corrected value of temperature in node  $x_i$ . From the balance of enthalpy:

$$\Delta H_i = \Delta H_{i1} + \Delta H_{i2}$$

we obtain the following formula for the corrected value of temperature in node  $x_i$ :

$$\bar{T}_i^{p+1} = T_L - \frac{C_l \rho_l}{C_{mz} \rho_{mz}} (T_L - T_i^{p+1})$$

In the similar way, we can derive the formula for the corrected value of temperature in case when node  $x_i$  passes from the mushy zone to the solid phase by obtaining:

$$\bar{T}_i^{p+1} = T_S - \frac{C_{mz} \rho_{mz}}{C_s \rho_s} (T_S - T_i^{p+1})$$

where  $C_s$  is the substantial thermal capacity of the solid phase and  $\rho_s$  – the density of the solid phase.

It is also possible to deduce the formula for the correction of temperature in case when node  $x_i$  passes immediately from the liquid phase to the solid phase, excluding the mushy zone. Anyway, it is better to select the length of time step,  $\Delta t$ , so that such situation will not happen.

In the next step of the procedure we compute the contribution of the solid phase in volume,  $V_j$ , in moment,  $t_{p+1}$ , by using relation (7) and we determine the locations of points  $\xi_i$  and  $\xi_s$ , bounding the liquid and solid phases, in the following way.

Let us select the nodes  $x_i$  and  $x_{i-1}$  for which  $T_i^{p+1} < T_L$  and  $T_{i-1}^{p+1} > T_L$  and let us provide the line through points  $(x_{i-1}, T_{i-1}^{p+1})$  and  $(x_i, T_i^{p+1})$ . Point  $x$  for which the line takes value  $T_L$  will be the sought point  $\xi_j$ . Thus we get:

$$\xi_l = x_{i-1} + \frac{x_{i-1} - x_i}{T_{i-1}^{p+1} - T_i^{p+1}} (T_L - T_{i-1}^{p+1})$$

Similarly we provide the line through points  $(x_{j-1}, T_{j-1}^{p+1})$  and  $(x_j, T_j^{p+1})$  for which  $T_j^{p+1} < T_S$  and  $T_{j-1}^{p+1} > T_S$ . Point  $x$  for which the line takes value  $T_S$  will be the sought point  $\xi_s$ , that is:

$$\xi_s = x_{j-1} + \frac{x_{j-1} - x_j}{T_{j-1}^{p+1} - T_j^{p+1}} (T_S - T_{j-1}^{p+1})$$

One step of calculations is ended by determining the width  $d(t)$  of the cast with the aid of eqs. (21) or (24).

### Numerical example

Let us consider a numerical example for verifying the elaborated procedure. We examine the problem of solidifying cast of length 0.4 m ( $d_0 = 0.4$ ) within the mould of length 0.2 m ( $b = 0.6$ ) described by the following sets of parameters [18]:

- for the liquid phase  
 $c_l = 1275 \text{ J/kgK}$ ,  $\rho_l = 2498 \text{ kg/m}^3$ ,  $\lambda_l = 183 \text{ W/mK}$ ,
- for the solid phase  
 $c_s = 1077 \text{ J/kgK}$ ,  $\rho_s = 2824 \text{ kg/m}^3$ ,  $\lambda_s = 183 \text{ W/mK}$ ,
- for the mould  
 $c_m = 620 \text{ J/kgK}$ ,  $\rho_m = 7500 \text{ kg/m}^3$ ,  $\lambda_m = 40 \text{ W/mK}$ .

Moreover, we take  $\alpha = 250 \text{ W/m}^2\text{K}$ ,  $L = 390000 \text{ J/kg}$ , liquidus and solidus temperatures  $T_L = 926 \text{ K}$  and  $T_S = 886 \text{ K}$ , ambient temperature  $T_\infty = 300 \text{ K}$ , initial temperature of the solidifying cast  $T_0 = 960 \text{ K}$ , initial temperature of the casting mould  $T_{m,0} = 590 \text{ K}$ , and thermal conductivity of the air gap  $\lambda_g = 15 \text{ W/mK}$ .

The calculations were executed for three variants of the velocity  $v_x$  included in the governing eq. (5):

- the velocity is non-zero in the solid phase and mushy zone where it is defined according to the following formulas:

$$v_x = \left( 1 - \frac{\bar{\rho}_{mz}}{\rho_s} \right) \frac{d\xi_s}{dt}$$

- in the mushy zone

$$v_x = \left( 1 - \frac{\rho_l}{\bar{\rho}_{mz}} \right) \frac{d\xi_l}{dt}$$

where  $\bar{\rho}_{mz}$  denotes the average density of mushy zone in the given moment of time;

- the velocity is non-zero only in the solid phase where it is determined by the relation:

$$v_x = \left( 1 - \frac{\rho_l}{\rho_s} \right) \frac{d\xi_s}{dt}$$

- the velocity is equal to zero in the entire considered domain.

It turned out that the results, obtained for these three variants of velocity variation, differ just slightly (we observed the differences only at the sixth decimal place), so we may con-

clude that in the considered problem, for the previous taken values of parameters, the velocity of the solidifying cast may not be taken into account.

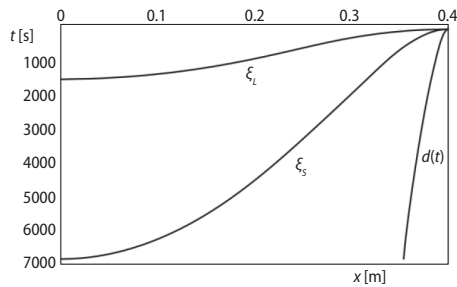


**Figure 2. Location of points  $\xi_l$  and  $\xi_s$ , bounding the liquid and solid phases in the cast, and point  $d(t)$ , denoting the cast boundary, during the solidification process**

Figure 2 displays the changes of locations of points  $\xi_l$  and  $\xi_s$  representing the liquidus and solidus temperatures  $T_L$  and  $T_S$ , respectively, as well as the location of point  $d(t)$  denoting the cast boundary, during the investigated solidification process. The figure shows that in moment 6870 seconds the whole cast is in the solid state, it means that the solidification ended in this moment. We may also observe the material shrinkage during the entire period of solidification.

In fig. 3 there are presented the distributions of temperature, in the cast and in the mould, in the selected moments of the solidification process, including time  $t = 6870$  of the final solidification.

Whereas, in fig. 4 there are collected the distributions of temperature in the selected moments of time after the final solidification time, that is during the process of the cast cooling. The obtained results are in line with our expectations.

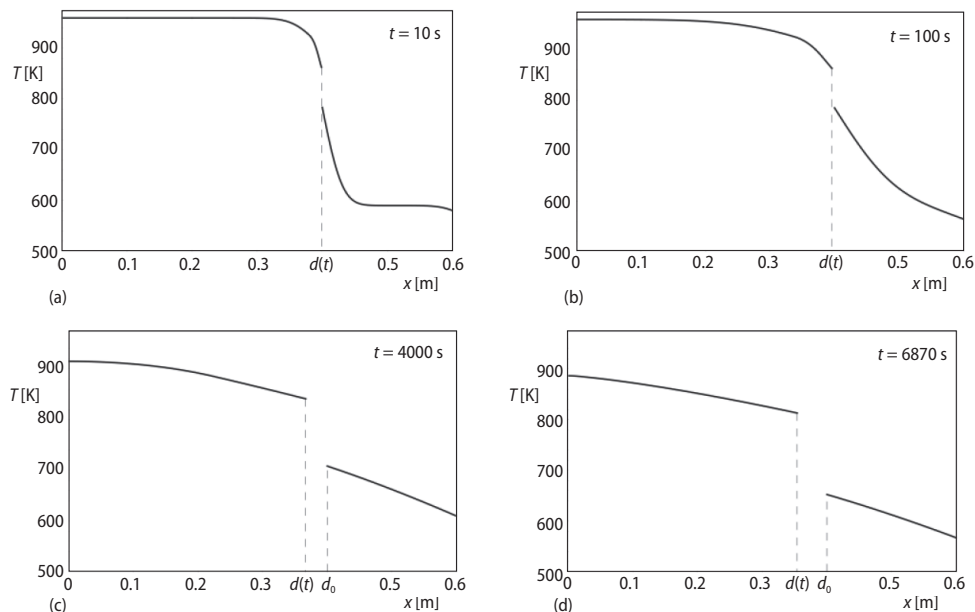


**Figure 3. Distributions of temperature, in the cast and in the mould, in the selected moments of time during the solidification process ( $t = 6870$  is the time of final solidification)**

Results presented in figs. 2-4 have been obtained for the calculations made for the number of nodes  $n = 2000$  for the cast and  $m = 600$  for the mould and for the time step  $\tau = 0.05$ . However, we decided to investigate more carefully the issue of the most effective grid. Therefore, we executed the calculations for various grids and we compared the results with the benchmark results (that is with the results received for  $n = 4000$ ,  $m = 1200$ , and  $\tau = 0.0005$ )



to answer the question how much we can reduce the number of nodes and the time step to keep the results at the acceptable level. In tabs. 1-3 there are compiled the maximal absolute, the maximal relative, and the average relative differences between the results obtained for the various grids and the results obtained for the benchmark grid in the selected moments of time. As a conclusion we may state that for the time step  $\tau = 0.02$  the results received for the grids  $n = 1000$ ,  $m = 300$  and  $n = 2000$ ,  $m = 600$  differ only slightly from the benchmark results, for the time step  $\tau = 0.05$  we should take the grid  $n = 2000$ ,  $m = 600$  to conclude the same, whereas the time step  $\tau = 0.1$  seems to be already to big. However, the more dense is the grid, the longer time is required to get the results. So, if for any reason we need to have some results very quickly, we may use a grid with time step  $\tau = 0.1$ , because even in this case the results are still tolerable.

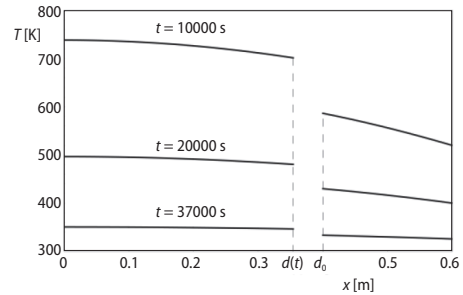


**Figure 4. Distributions of temperature, in the cast and in the mould, in the selected moments of time during the process of the cast cooling**

**Table 1. Maximal absolute,  $\Delta T$ , maximal relative,  $\delta T$ , and average relative,  $\delta T_{avg}$  differences between the temperature calculated for the benchmark grid and the given grids for time step  $\tau = 0.02$  in the selected moments of time**

$n$ (cast)	500			1000			2000		
$m$ (mould)	150			300			600		
$t$ [s]	$\Delta T$ [K]	$\delta T$ [%]	$\delta T_{avg}$ [%]	$\Delta T$ [K]	$\delta T$ [%]	$\delta T_{avg}$ [%]	$\Delta T$ [K]	$\delta T$ [%]	$\delta T_{avg}$ [%]
10	19.059	2.433	0.188	1.818	0.236	0.022	2.052	0.269	0.024
100	5.444	0.695	0.186	0.414	0.054	0.018	1.013	0.129	0.025
1000	1.336	0.176	0.087	0.360	0.039	0.008	0.285	0.038	0.020
4000	3.754	0.410	0.215	0.996	0.109	0.065	0.122	0.017	0.009
6850	10.054	1.14	0.786	2.779	0.314	0.219	0.275	0.031	0.006
10000	10.931	1.482	1.219	2.617	0.355	0.295	0.087	0.012	0.009
20000	4.785	0.964	0.800	1.149	0.232	0.193	0.037	0.008	0.006
37000	1.233	0.352	0.281	0.296	0.084	0.068	0.010	0.003	0.002

**Table 2. Maximal absolute,  $\Delta T$ , maximal relative,  $\delta T$ , and average relative,  $\delta T_{avg}$  differences between the temperature calculated for the benchmark grid and the given grids for time step  $\tau = 0.05$  in the selected moments of time**

$n$ (cast)	500			1000			2000		
$m$ (mould)	150			300			600		
$t$ [s]	$\Delta T$ [K]	$\delta T$ [%]	$\delta T_{avg}$ [%]	$\Delta T$ [K]	$\delta T$ [%]	$\delta T_{avg}$ [%]	$\Delta T$ [K]	$\delta T$ [%]	$\delta T_{avg}$ [%]
10	2.546	0.316	0.035	7.140	1.065	0.163	2.660	0.306	0.053
100	1.038	0.108	0.025	2.334	0.302	0.140	1.815	0.232	0.058
1000	0.724	0.078	0.026	1.294	0.172	0.089	0.755	0.099	0.053
4000	1.900	0.208	0.122	0.389	0.055	0.030	0.559	0.079	0.047
6850	4.631	0.525	0.373	0.708	0.081	0.018	0.697	0.081	0.036
10000	4.696	0.637	0.528	0.096	0.013	0.007	1.058	0.143	0.119
20000	2.063	0.416	0.346	0.043	0.009	0.0044	0.094	0.464	0.078
37000	0.531	0.152	0.122	0.011	0.003	0.002	0.119	0.034	0.027

**Table 3. Maximal absolute,  $\Delta T$ , maximal relative,  $\delta T$ , and average relative,  $\delta T_{avg}$  differences between the temperature calculated for the benchmark grid and the given grids for time step  $\tau = 0.1$  in the selected moments of time**

$n$ (cast)	500			1000			2000		
$m$ (mould)	150			300			600		
$t$ [s]	$\Delta T$ [K]	$\delta T$ [%]	$\delta T_{avg}$ [%]	$\Delta T$ [K]	$\delta T$ [%]	$\delta T_{avg}$ [%]	$\Delta T$ [K]	$\delta T$ [%]	$\delta T_{avg}$ [%]
10	6.940	0.888	0.073	8.858	1.144	0.182	6.538	0.869	0.083
100	2.187	0.280	0.071	2.961	0.382	0.162	2.503	0.320	0.081
1000	0.669	0.088	0.046	1.688	0.219	0.115	1.034	0.137	0.072
4000	0.890	0.097	0.036	0.878	0.124	0.065	0.797	0.113	0.066
6850	2.741	0.311	0.182	0.196	0.022	0.005	0.906	0.106	0.043
10000	2.010	0.273	0.228	1.033	0.140	0.113	1.417	0.192	0.161
20000	0.888	0.179	0.149	0.452	0.091	0.074	0.625	0.126	0.104
37000	0.229	0.065	0.052	0.116	0.033	0.026	0.161	0.046	0.036

## Conclusions

Aim of this paper was to present the solution method for the direct alloy solidification problem taking into account the air gap formed between the cast and the mould. Mathematically the process was modeled by means of the so-called solidification in the temperature interval, that is with the aid of the heat conduction equation with the substitute thermal capacity describing the distribution of temperature in the solid phase, two-phase zone, and liquid phase. Whereas the phenomenon of material shrinkage was modeled by the proper application of the mass balance equation.

Goal of the described procedure was to determine the temperature distribution in the investigated domain including the region of the ingot and the region of the casting mould, as well as the change of cast size caused by the material shrinkage. The calculations were performed for three variants of the velocity included in the governing equation and for various grids introduced in the considered domain to examine the influence of the grid density on the quality of results. Obtained results are very satisfying, considering their quality as well as the fastness of the procedure, so they are very promising for the future since we plan to use the developed procedure in solving the appropriate inverse problems.

## Nomenclature

$b$  – length, [m]  
 $C$  – substitute thermal capacity, [ $\text{Jkg}^{-1}\text{K}^{-1}$ ]  
 $c$  – specific heat, [ $\text{Jkg}^{-1}\text{K}^{-1}$ ]  
 $d$  – thickness of the plate, [m]  
 $f_s$  – volumetric solid state fraction, [–]  
 $\Delta H_i$  – change of enthalpy, [J]  
 $h$  – height of the plate, [m]  
 $k$  – step of the mesh, [–]  
 $L$  – latent heat of solidification, [ $\text{Jkg}^{-1}$ ]  
 $l$  – width of the plate, [m]  
 $m$  – mass of the alloy, [kg]  
 $n$  – number of nodes, [–]  
 $R$  – thermal resistance, [ $\text{m}^2\text{KW}^{-1}$ ]  
 $T$  – temperature, [K]  
 $T_L$  – liquidus temperature, [K]  
 $T_S$  – solidus temperature, [K]

$T_\infty$  – ambient temperature, [K]  
 $t$  – time, [s]  
 $t^*$  – final time, [s]  
 $V_j$  – control volume, [ $\text{m}^3$ ]  
 $v_x$  – velocity, [ $\text{ms}^{-1}$ ]  
 $x$  – spatial variable, [–]

### Greek symbols

$\alpha$  – heat transfer coefficient, [ $\text{Wm}^{-2}\text{K}^{-1}$ ]  
 $\delta$  – relative percentage error, [%]  
 $\Delta$  – absolute error, [–]  
 $\lambda$  – thermal conductivity, [ $\text{Wm}^{-1}\text{K}^{-1}$ ]  
 $\rho$  – mass density, [ $\text{kgm}^{-3}$ ]  
 $\tau$  – time step, [–]  
 $\xi_{L(s)}$  – location of  $T_{L(s)}$ , [m]  
 $\Omega$  – considered region, [–]

*Subscripts*

$l$  – liquid phase  
 $m$  – mould

$mz$  – mushy zone  
 $s$  – solid phase  
 $0$  – initial

**References**

- [1] Nawrat, A., Skorek, J., Inverse Finite Element Technique for Identification of Thermal Resistance of Gas-Gap between the Ingot and Mould in Continuous Casting of Metals, *Inverse Probl. Sci. Eng.*, 12 (2004), 2, pp. 141-155
- [2] Nawrat, A., *et al.*, Identification of the Heat Fluxes and Thermal Resistance on the Ingot-Mould Surface in Continuous Casting of Metals, *Inverse Probl. Sci. Eng.*, 17 (2009), 3, pp. 399-409
- [3] Grzymkowski, R., *Inverse Problems in Thermodynamics of the Foundry Processes* (in Polish), Silesian University of Technology Press, Gliwice, Poland, Mechanics, 91, 1991
- [4] Shestakov, N. I., *et al.*, Heat Exchange Regularities in a Crystallizer, *Izv. V.U.Z. Chernaya Metall.*, 1 (1994), pp. 22-23
- [5] Cheung, N., *et al.*, Interfacial Heat Transfer Coefficients and Solidification of an Aluminum Alloy in a Rotary Continuous Caster, *Int. J. Heat Mass Transfer*, 52 (2009), 1-2, pp. 451-459
- [6] O'Mahoney, D., Browne, D. J., Use of Experiment and an Inverse Method to Study Interface Heat Transfer During Solidification in the Investment Casting Process, *Exp. Therm. Fluid Sci.*, 22 (2000), 3-4, pp. 111-122
- [7] Matlak, J., Slota, D., Solution of the Pure Metals Solidification Problem by Involving the Material Shrinkage and the Air-Gap Between Material and Mold, *Arch. Foundry Eng.*, 15 (2015), spec., 4, pp. 47-52
- [8] Matlak, J., Slota, D., Solution of the Stefan Problem by Involving the Material Shrinkage, *Technical Transactions, 2-M* (2015), pp. 157-164
- [9] Gupta, S. C., *The Classical Stefan Problem. Basic Concepts, Modelling and Analysis*, Elsevier, Amsterdam, 2003
- [10] Hetmaniok, E., *et al.*, Using the Swarm Intelligence Algorithms in Solution of the Two-Dimensional Inverse Stefan Problem, *Comput. Math. Appl.*, 69 (2015), 4, pp. 347-361
- [11] Hristov, J., An Inverse Stefan Problem Relevant to Boilover: Heat Balance Integral Solutions and Analysis, *Thermal Science*, 11 (2007), 2, pp. 141-160
- [12] Ionescu, D., *et al.*, 2D Mathematical Model for the Solidification of Alloys within a Temperature Interval, *Metalurgia International*, 16 (2011), 4, pp. 39-44
- [13] Szopa, R., *Sensitivity Analysis and Inverse Problems in Thermodynamics of Foundry Processes* (in Polish), Czestochowa University of Technology Press, Czestochowa, Poland, 2006
- [14] Mochnacki, B., Numerical Modeling of Solidification Process, in: *Computational Simulations and Applications*, (Ed. J. Zhu), InTech, Rijeka, Croatia, 2011, pp. 513-542
- [15] Mochnacki, B., Suchy, J. S., *Numerical Methods in Computations of Foundry Processes*, PFTA, Cracow, Poland, 1995
- [16] Majchrzak, E., Mochnacki, B., Application of the BEM in the Thermal Theory of Foundry, *Eng. Anal. Bound. Elem.*, 16 (1995), 2, pp. 99-121
- [17] Szargut, J., Mochnacki, B., Difference Mathematical Model of Ingot Solidification, *Arch. Hutn.*, 16 (1971), 3, pp. 269-289
- [18] Szczygiol, N., *Numerical Modeling of Thermo-Mechanical Phenomena in Solidifying Cast and Casting Mould* (in Polish), Czestochowa University of Technology Press, Czestochowa, Poland, 2000